



# Martensitic transformation, mechanical property and magnetic-field-induced strain of Ni–Mn–Ga alloy fabricated by spark plasma sintering

X.H. Tian<sup>a,b</sup>, J.H. Sui<sup>a</sup>, X. Zhang<sup>a</sup>, X. Feng<sup>a</sup>, W. Cai<sup>a,\*</sup>

<sup>a</sup> National key Laboratory Precision Hot Processing of Metals, School of Materials Science and Engineering, Harbin Institute of Technology, Harbin 150001, China

<sup>b</sup> School of Applied Science, Harbin University of Science and Technology, Harbin 150080, China

## ARTICLE INFO

### Article history:

Received 1 December 2010

Received in revised form

29 December 2010

Accepted 3 January 2011

Available online 8 January 2011

### Keywords:

Ferromagnetic shape memory alloys

Phase transitions

Mechanical property

Sintering

## ABSTRACT

Martensitic transformation, mechanical property and magnetic-field-induced strain of Ni–Mn–Ga alloys obtained using the spark plasma sintering method have been investigated. The results show that the martensitic transformation of the sintered specimen is basically similar to that of conventional bulk alloys. The ductility of sintered Ni–Mn–Ga alloys is significantly enhanced compared to the specimen obtained by conventional melting technique. The highest fracture strain so far is reported. Moreover, magnetic-field-induced strain in sintered Ni–Mn–Ga alloys has been studied for the first time.

© 2011 Elsevier B.V. All rights reserved.

## 1. Introduction

Ni–Mn–Ga alloy has attracted considerable attention in recent years because it exhibits both ferromagnetism and shape memory effect [1–5]. The large magnetic-field-induced strain (MFIS) of up to 10% has been reported in Ni–Mn–Ga [6]. This makes it an ideal candidate for magnetically controlled shape memory application. Such large MFIS is based on a rearrangement of martensite variants by an external magnetic field induced by a strong coupling between magnetic and mechanical variables. So far, although Ni–Mn–Ga alloy has been extensively studied, there are some problems in the application. Significant brittleness of the Ni–Mn–Ga alloys is a serious problem preventing application of this material. To overcome the brittleness of the bulk alloy, several forms based on the alloy have been developed, including ribbons and thin films [7–10]. However, although the ductility is expected to be improved by these methods, the shape of specimens is limited and the fabrication of bulk specimens with a relatively large size is difficult.

On the other hand, powder metallurgy is one of the most effective techniques for improving the ductility of bulk specimens. It has been demonstrated that powder metallurgy improves not only ductility but also shape memory properties of Cu–Al–Ni shape memory alloy [11,12]. In particular, the spark plasma sintering (SPS) technique

is designed to sinter metal powder in a short time to achieve dense materials. High speed sintering is of particular advantage to achieve fine grains and dense structures, which leads to high toughness and strength. Until now, only few investigations on sintered Ni–Mn–Ga ferromagnetic shape memory alloys fabricated by the SPS technique have been reported [13,14]. Little information about the MFIS in sintered Ni–Mn–Ga alloys has been found to date despite its importance. Moreover, the martensitic transformation and mechanical property of sintered Ni–Mn–Ga alloys need extensive studies. Thus, the purpose of this paper is to investigate the microstructure, martensitic transformation and mechanical property of Ni–Mn–Ga alloys fabricated by the SPS method. Furthermore, the MFIS in SPS-sintered Ni–Mn–Ga alloys has been studied for the first time. The results show that the ductility of Ni–Mn–Ga alloys is significantly enhanced by powder metallurgy using the SPS technique.

## 2. Experimental

A Ni<sub>48.8</sub>Mn<sub>29.7</sub>Ga<sub>21.5</sub> alloy was prepared with high-purity elements melted four times in an arc-melting furnace under an argon atmosphere. The arc-melted alloy was sealed in quartz tube under a vacuum, then annealed at 1073 K for 24 h and quenched into iced water for homogeneity. Part of the annealed arc-melted alloy was machined for property comparison with sintered specimens. The remainder was mechanically crushed and followed by ball milling to achieve powder. Subsequently, the obtained powder was sintered by the SPS technique, sintering being performed at 1173 K for 10 min in a vacuum of 6 Pa under a pressure of 50 MPa in a graphite die. The as-sintered alloys were then annealed at 1073 K for 12 h in quartz tube under a vacuum. X-ray diffraction (XRD) measurements were performed to determine the crystal structure using a Rigaku D/max-rB with Cu K $\alpha$  radiation. Microstructures of the specimens were studied in a MX2600FE scanning electron microscopy analysis

\* Corresponding author. Tel.: +86 451 86418649; fax: +86 451 86415083.

E-mail addresses: [xiaohuatian@yahoo.com.cn](mailto:xiaohuatian@yahoo.com.cn) (X.H. Tian), [weicai@hit.edu.cn](mailto:weicai@hit.edu.cn) (W. Cai).

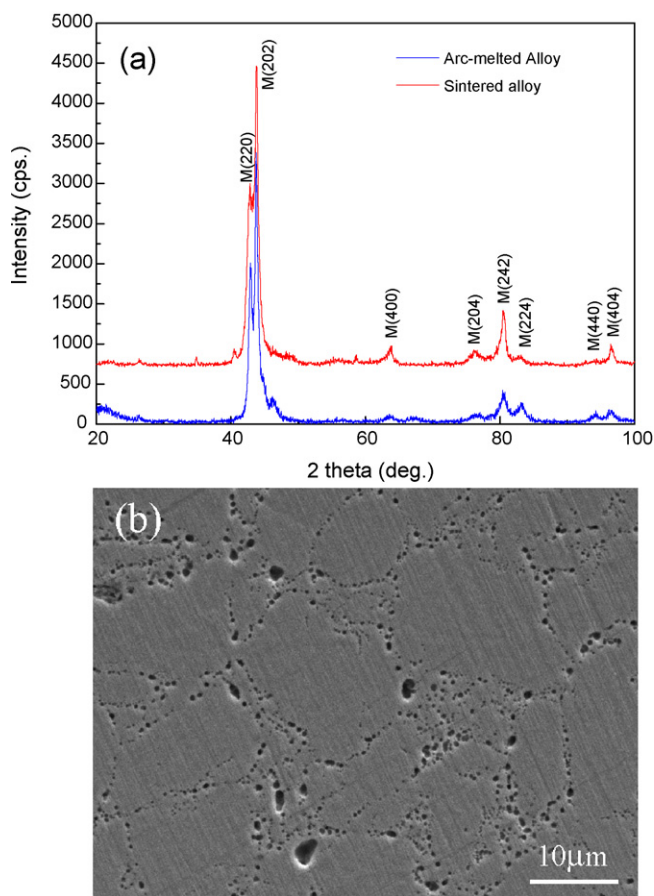


**Fig. 1.** (a) XRD patterns of the sintered and arc-melted Ni–Mn–Ga alloys. (b) Microstructure of the sintered Ni–Mn–Ga alloy.

system. The martensitic transformation temperatures and the Curie temperature were determined by low-field ac magnetic susceptibility for the arc-melted and sintered specimens with a rectangular shape of about  $2 \times 2 \times 1 \text{ mm}^3$ . Compression testing was conducted at ambient temperature on an Instron-1186 machine at a strain rate of  $0.05 \text{ mm min}^{-1}$  using the arc-melted and sintered specimens with a rectangular shape of about  $3 \times 3 \times 5 \text{ mm}^3$ . The MFIS was measured by standard strain gauge techniques. Samples with dimension of  $4 \times 3 \times 2 \text{ mm}^3$  were cut for the measurement of the MFIS.

### 3. Results and discussion

Fig. 1(a) illustrates the room temperature XRD patterns of the sintered and arc-melted Ni–Mn–Ga alloys. The XRD pattern of the sintered specimen maintains the same crystal structure as the arc-melted specimen. The typical martensite peaks can be seen clearly in both studied alloys. According to the XRD results, the crystal structures can be indexed by the five-layer tetragonal martensite with the lattice parameters  $a = b = 0.595 \text{ nm}$  and  $c = 0.548 \text{ nm}$  for the sintered alloy,  $a = b = 0.594 \text{ nm}$  and  $c = 0.550 \text{ nm}$  for the arc-melted alloy, respectively. Previous studies [13] show that the as-sintered Ni–Mn–Ga alloys exhibit the broadened XRD peaks. Such broadening arises from the simultaneous variation of lattice strain and grain size, which is due to the grinding-induced stress. Compared to the as-sintered alloy, narrower XRD peaks in our studied sintered specimen annealed at 1073 K indicate that larger grain size and lower lattice strain have been produced.

Fig. 1(b) shows the microstructure of the sintered Ni–Mn–Ga alloy. It is apparent that the sintered specimen has a single-phase structure without any large second-phase regions. Moreover, it can be seen that only a small amount of fine pores is observed in the specimen sintered at 1173 K. This indicates that the sintering tem-

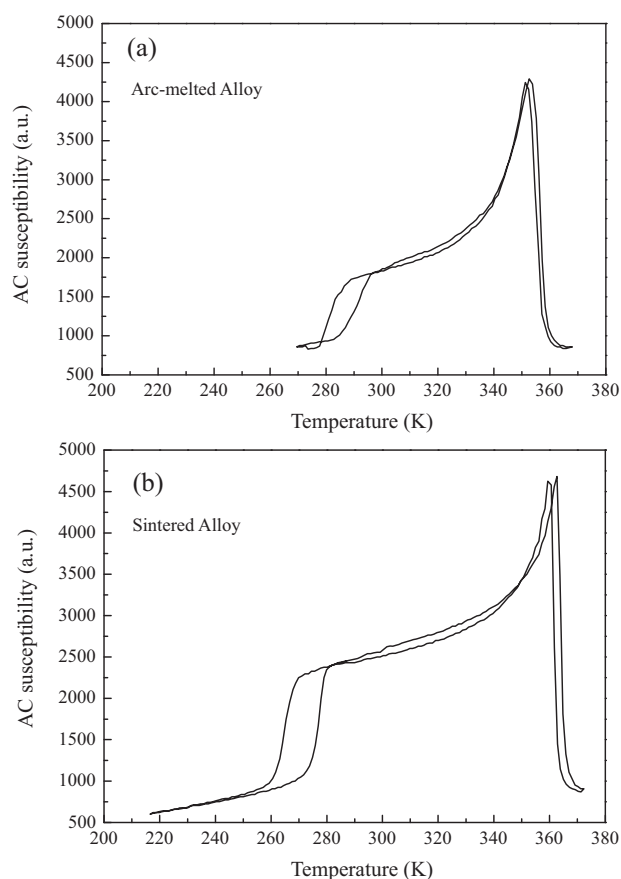


**Fig. 2.** Temperature dependencies of low-field ac magnetic susceptibility of the sintered and arc-melted Ni–Mn–Ga alloys during heating and cooling.

perature of 1173 K is sufficient to obtain a high density. The average grain size of the sintered specimen is about  $12 \mu\text{m}$ . The grain size of the arc-melted alloy is much bigger than that of the sintered alloy because the SPS technique achieves refined grains.

Fig. 2 shows the temperature dependencies of low-field ac magnetic susceptibility of the sintered and arc-melted Ni–Mn–Ga alloys during heating and cooling. It is found that there are characteristically two abrupt changes in such susceptibility curves for both specimens, corresponding to the martensitic transformation and magnetic transition, respectively. This indicates that the sintered specimen maintains the characteristics of the typical one-step thermoelastic martensitic transformation of the arc-melted Ni–Mn–Ga alloy. Moreover, it can be seen that the martensitic and reverse transformation temperatures of the sintered specimen decrease compared to those of the arc-melted specimen. It is known that the martensitic transformation temperatures of Ni–Mn–Ga alloys are sensitive to the grain size. Small grain size would result in the decrease of martensitic transformation temperature in ferromagnetic shape memory alloys [15]. Therefore, it can be concluded that a reduction of the grain size in our studied sintered specimen causes a decrease in the martensitic transformation temperature. In addition, from Fig. 2, it can be obviously seen that for the sintered specimen, the Curie temperature is higher than the martensitic transformation temperature. This implies that the martensitic phase is ferromagnetic nature, which is the basic condition for observation of MFIS in ferromagnetic shape memory alloys.

In order to investigate the ductility of the sintered and arc-melted specimens, compression tests were carried out at room temperature. Both specimens were compressed to fracture. Fig. 3 shows the compressive stress-strain curves at room temperature

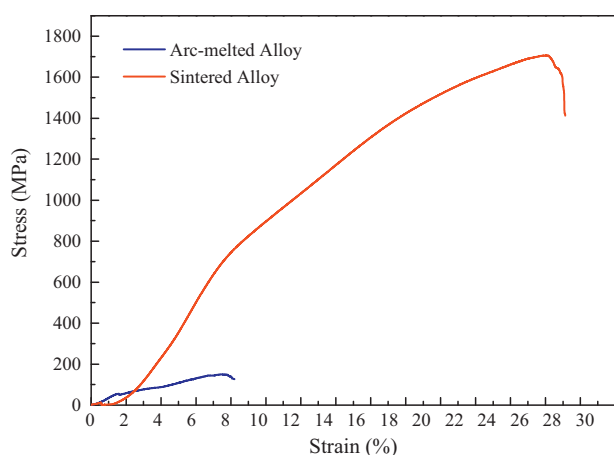


Fig. 3. Compressive stress-strain curves of the sintered and arc-melted Ni–Mn–Ga alloys at room temperature.

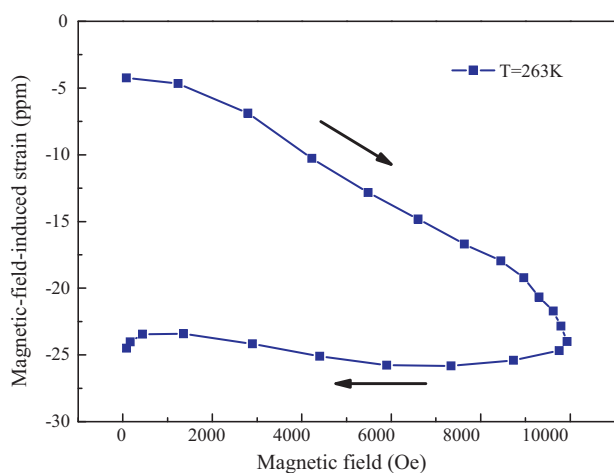


Fig. 4. MFIS in the SPS-sintered Ni–Mn–Ga alloy at 263 K.

obtained from the sintered specimen in comparison with that from the arc-melted specimen. It can be seen that the arc-melted specimen is subject to 8% fracture strain. On the other hand, in the sintered specimen, the fracture occurred at a strain of about 27%. This is the highest fracture strain reported to date in the Ni–Mn–Ga alloy system. Moreover, the compressive strength of 1706 MPa is obtained for the sintered specimen, which is significantly higher than that of the arc-melted specimen. Therefore, both the compressive strength and fracture strain of the sintered specimen are higher than those of the arc-melted specimen. This clearly demonstrates that the ductility of Ni–Mn–Ga alloys is significantly enhanced by powder metallurgy using the SPS technique. The enhancement of the ductility for the sintered specimen may be attributed to the strengthening of grain boundaries and reduction of the grain size, which has been reported in Cu–Al–Ni alloys [12].

Fig. 4 shows the result of the MFIS measurements in the sintered specimen at 263 K. A MFIS of  $-20$  ppm has been obtained. This MFIS remains after removing the magnetic field. It is obviously found that the obtained MFIS is low and comparable to that of the polycrystalline bulk alloy and ribbon [7]. On the other hand,

it is worth noting that the dense sintered specimen is composed of the grains perfectly surrounded by neighboring grains. Thus, the low MFIS may be due to the incompatibilities across the grain boundaries and limited martensite reorientation caused by the geometric constraints from surrounding grains during deformation. Recently, it has been reported that introducing pores in polycrystalline Ni–Mn–Ga drastically increases its MFIS by reducing the effect of constraints imposed by grain boundaries and thus enabling twin boundary motion [16,17]. Therefore, we infer that introducing appropriate pores in the sintered Ni–Mn–Ga alloys would make this material exhibit both high ductility and large MFIS.

#### 4. Conclusions

In summary, for Ni–Mn–Ga alloys fabricated by the SPS method, the microstructure, martensitic transformation and mechanical property as well as MFIS have been investigated. The results show that the sintered specimen maintains the characteristics of the typical one-step thermoelastic martensitic transformation of the arc-melted Ni–Mn–Ga alloy, while its martensitic and reverse transformation temperatures decrease owing to the reduction of the grain size. The ductility of sintered Ni–Mn–Ga alloys is significantly enhanced compared to the specimen obtained by conventional melting technique. In particular, the highest fracture strain of 27% up to now has been reported. In addition, the magnetic-field-induced strain in sintered Ni–Mn–Ga alloys has been obtained for the first time, which is relatively low due to constraints imposed by grain boundaries in the dense structure.

#### Acknowledgement

This work is supported by National Natural Science Foundation of China (Grant nos. 50971052, 50801018 and 51071059).

#### References

- [1] K. Ullakko, J.K. Huang, C. Kantner, R.C. O'Handley, V.V. Kokorin, *Appl. Phys. Lett.* 69 (1996) 1966–1968.
- [2] V.A. Chernenko, E. Cesari, V.V. Kokorin, I.N. Vitenko, *Scripta Metall. Mater.* 33 (1995) 1239–1244.
- [3] J. Pons, V.A. Chernenko, R. Santamarta, E. Cesari, *Acta Mater.* 48 (2000) 3027–3038.
- [4] S.J. Murray, M.A. Marioni, S.M. Allen, R.C. O'Handley, T.A. Lograsso, *Appl. Phys. Lett.* 77 (2000) 886–888.
- [5] G.H. Wu, C.H. Yu, L.Q. Meng, *Appl. Phys. Lett.* 75 (1999) 2990–2992.
- [6] A. Sozinov, A.A. Likhachev, N. Lanska, K. Ullakko, *Appl. Phys. Lett.* 80 (2002) 1746–1748.
- [7] N.V. Rama Rao, R. Gopalan, M. Manivel Raja, J. Arout Chelvance, B. Majumdar, V. Chandrasekaran, *Scripta Mater.* 56 (2007) 405–408.
- [8] A.K. Panda, M. Ghosh, A. Kumar, A. Mitra, *J. Magn. Magn. Mater.* 320 (2008) L116–L120.
- [9] Y. Feng, J.H. Sui, L. Chen, W. Cai, *Mater. Lett.* 63 (2009) 965–968.
- [10] C.A. Jenkins, R. Ramesh, M. Huth, T. Eichhorn, P. Porsch, H.J. Elmers, G. Jakob, *Appl. Phys. Lett.* 93 (2008) 234101.
- [11] T.W. Duering, J. Albrecht, G.H. Gessinger, *J. Met.* 34 (1982) 14–20.
- [12] R.B. Pérez-Sáez, V. Recarte, M.L. Nó, O.A. Ruano, J. San Juan, *Adv. Eng. Mater.* 2 (2000) 49–53.
- [13] Z. Wang, M. Matsumoto, T. Abe, K. Oikawa, J.H. Qiu, T. Takagi, J. Tani, *Mater. Trans. JIM* 40 (1999) 389–391.
- [14] T. Takagi, V. Khovailo, T. Nagatomo, M. Matsumoto, M. Ohtsuka, T. Abe, H. Miki, *Int. J. Appl. Electr. Mech.* 16 (2002) 173–179.
- [15] K. Seki, H. Kura, T. Sato, T. Taniyama, *J. Appl. Phys.* 103 (2008) 063910.
- [16] M. Chmielus, X.X. Zhang, C. Witherspoon, D.C. Dunand, P. Müllner, *Nat. Mater.* 8 (2009) 863–866.
- [17] Y. Boonyongmaneerat, M. Chmielus, D.C. Dunand, P. Müllner, *Phys. Rev. Lett.* 99 (2007) 247201.